

Probabilistic properties of wavelets in kinetic surface roughening

A. Bershadskii

ICAR, P.O. Box 31155, Jerusalem 91000, Israel

(Received 17 January 2001; published 23 July 2001)

Using the data of a recent numerical simulation [M. Ahr and M. Biehl, Phys. Rev. E **62**, 1773 (2000)] of homoepitaxial growth it is shown that the observed probability distribution of a wavelet based measure of the growing surface roughness is consistent with a stretched log-normal distribution and the corresponding branching dimension depends on the level of particle desorption.

DOI: 10.1103/PhysRevE.64.027104

PACS number(s): 64.60.Ht, 05.40.-a, 81.10.Aj

I. INTRODUCTION

In recent years different physical and mathematical ideas and methods have been applied to study problems of epitaxial crystal growth that are important for modern technology. From the physical point of view it is an interesting example of phenomena far from thermal equilibrium (see, for instance, [1] and references therein), and the recently discovered remarkable analogy with fluid turbulence [2,3] allows the application of ideas and methods used in that field to explore it. In particular, extended self-similarity, which was discovered in fluid turbulence, was then successfully used to study kinetic surface roughening [2]. The wavelet transform modulus maxima method, also applied to processes related to turbulence, was recently used in the field of rough growing surfaces [4,5]. The nature of extended self-similarity in turbulence itself is still unclear. In a recent paper [6] the appearance of extended self-similarity in turbulence is related to log-normal-like processes. Numerical simulations performed in [6] show the log-normal-like behavior in a very wide interval of scales (including the so-called viscous interval). Due to the strong influence of molecular diffusion on motion in the viscous interval of scales the simple multiplicative splitting of eddies (inviscid cascade [7]) cannot be realized in this interval of scales [7,8], and the direct relation of log-normal-like behavior to simple cascade processes becomes questionable. Therefore, one might expect that a more sophisticated process (e.g., a branching cascade [11]) is responsible for the log-normal-like behavior when molecular diffusion effects become significant. This observation and the above mentioned analogy between kinetic surface roughening and fluid turbulence allows us to seek evidence of log-normal-like distributions related to branching cascade processes in kinetic surface roughening as well.

Usually, we have two main problems in identifying relevant probabilistic properties of space-extended stochastic systems. First of all there is the problem of choosing an adequate measure and the second problem is to identify the probability density function corresponding to this measure. For some scale-invariant systems the method of moments can be used to solve (in some sense) the second problem. However, when we are dealing with moments the first problem becomes even more difficult. Indeed, the height-height correlation functions of an arbitrary order p

$$c_p(r, t) = \langle |h(\mathbf{x}, t) - h(\mathbf{x} + \mathbf{r}, t)|^p \rangle \quad (1)$$

are usually used in the method of moments. However, it is now well known that the correlation function method can easily be corrupted by polynomial trends in $h(\mathbf{x})$ [9]. Therefore, a different method (the so-called wavelet transform modulus maxima method) was recently developed to avoid this (and some other) problems [4] and then this method was successfully applied to the kinetic surface roughening problem [5]. In this method the wavelet transform of a function $h(\mathbf{x})$ is defined as its convolution with the complex conjugate of the wavelet ψ , which is dilated with the scale r and rotated by an angle Θ :

$$M_\psi(h, \mathbf{b}, r) \sim r^{-2} \int d^2x \psi^* [r^{-1} \mathbf{R}_{-\Theta}(\mathbf{x} - \mathbf{b})] h(\mathbf{x}), \quad (2)$$

where \mathbf{R}_Θ is the usual two-dimensional rotation matrix. The wavelet can (in principle) be an arbitrary normalized function. In particular, the wavelet

$$\psi_\delta(\mathbf{x}) = \delta(\mathbf{x}) - \delta(\mathbf{x} + \mathbf{n})$$

(where \mathbf{n} is an arbitrary unit vector) leads to

$$M_\psi(h, r) \sim h(\mathbf{b}) - h(\mathbf{b} + r\mathbf{R}_\Theta\mathbf{n}).$$

That is, in this particular case we return to the usual correlation function moments

$$c_p(r\mathbf{R}_\Theta\mathbf{n}) \sim \int d\mathbf{b} |M_\psi(h, r)|^p.$$

To avoid the weakness of the correlation function method a more complex wavelet can be used. In particular, in Ref. [5] Gaussian based wavelets were successfully used. Then, the wavelet transform modulus maxima (WTMM) are defined as local maxima of the modulus $|M_\psi(h, r)|$ for fixed r . These wavelet transform modulus maxima lie on connected curves, which trace structures of size $\sim r$ on the surface. The strength of each is characterized by the maximal value of $|M_\psi(h, r)|$ along the line, the so-called wavelet transform modulus maxima maximum (WTMMM). When proceeding from large to small r , successively smaller structures are resolved. Connecting the WTMMM at different scales yields the set $L(r)$ of maxima lines l , which leads to the locations of the singularities of $h(\mathbf{x})$ in the limit $r \rightarrow 0$.

Scaling of the partition function

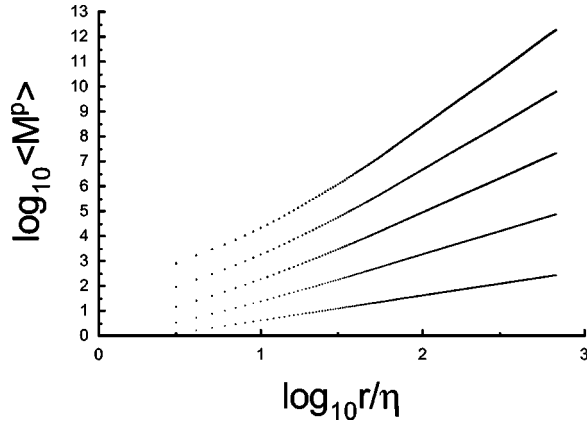


FIG. 1. $\langle M^p \rangle$ versus r/η for $p=1,2,3,4,5$ (upper sets of data correspond to larger values of p ; η is a molecular scale).

$$Z_p = \sum_{l \in L} \left(\sup_{(\mathbf{b}, r') \in l, r' \leq r} |M_{\psi}(h, \mathbf{b}, r')| \right)^p \sim r^{\tau_p} \quad (3)$$

for $r \rightarrow 0$ is defined on the subset $L(r)$ of lines that cross the scale r . Since $-\tau_0$ can be identified as the dimension of the set of singularities of $h(\mathbf{x})$ we can define the scaling of the corresponding wavelet moments as

$$\langle M^p \rangle \sim r^{-\tau_0} Z_p \sim r^{\tau_p - \tau_0} \quad (4)$$

and then define the wavelet generalized Hurst exponents as

$$H_p^w = \frac{(\tau_p - \tau_0)}{p}. \quad (5)$$

Figure 1 shows the typical dependence of the moments $\langle M^p \rangle$ on r .

II. MODEL

In Ref. [5] a full-diffusion Monte Carlo model of homoepitaxial growth of a material with simple cubic lattice structure under solid on solid conditions was investigated using the wavelet transform modulus maxima maximum method. In this model the crystal can be described by a two-dimensional array of integers that denote the height $h(\mathbf{x})$ of the surface. The authors of Ref. [5] simulated the deposition of 2×10^4 monolayers at a growth rate of one monolayer per second on a lattice of 512×512 unit cells using periodic boundary conditions. Particles on the surface hop to nearest neighbor sites with Arrhenius rates $\nu_0 \exp[-(E_b + nE_n)/k_b T]$, where E_b and E_n are the binding energies of a particle to the substrate and to its n nearest neighbors, and ν_0 is the attempt frequency. In contrast to earlier investigations of similar models [10], in the investigation performed in Ref. [5] the desorption of particles from the surface with rates $\nu_0 \exp[-(E_d + nE_n)/(k_b T)]$ (where $E_d > E_b$) was permitted. The authors of Ref. [5] chose parameters $E_b = 0.9$ eV and $E_n = 0.25$ eV, $\nu_0 = 10^{12}$ /s, and $T = 450$ K to calculate the exponent τ_p for several values of E_d .

III. STRETCHED LOG-NORMAL DISTRIBUTION

It is shown in Ref. [9] that the central limit theorem (which results in the log-normal distribution for the ordinary cascade models) applied to fractals leads to a generalization of the normal distribution, the *stretched* normal distribution and, consequently, to the stretched log-normal distribution for branching cascades on fractals. The stretched normal distribution has the form

$$P(M) \sim \exp\left(-\frac{|M - M_c|^{2d}}{2\sigma^2}\right), \quad (6)$$

where σ and M_c are some parameters and d is the branching dimension [11]. The corresponding stretched log-normal distribution is

$$P(M) \sim \frac{1}{M} \exp\left(-\frac{|\ln M - \ln M_c|^{2d}}{2\sigma^2}\right). \quad (7)$$

The moments corresponding to the stretched log-normal distribution can be estimated as

$$\langle M^p \rangle \sim \int_0^\infty M^p \exp\left(-\frac{|\ln M - \ln M_c|^{2d}}{2\sigma^2}\right) \left(\frac{1}{M} dM\right). \quad (8)$$

Let introduce the variable

$$x = \ln M - \ln M_c. \quad (9)$$

Then

$$\langle M^p \rangle \sim e^{ap} \int_{-\infty}^\infty \exp\left(px - \frac{|x|^{2d}}{2\sigma^2}\right) dx. \quad (10)$$

We denote

$$f(x) = px - \frac{|x|^{2d}}{2\sigma^2} \quad (11)$$

and find the value of x where this function has its maximum using the equation

$$f'(x) = p - \frac{d}{\sigma^2} |x|^{2d-1} = 0 \quad (12)$$

($p > 0$). Equation (12) has the solution

$$x_0 = \left(\frac{\sigma^2 p}{d}\right)^\alpha, \quad (13)$$

where

$$\alpha = \frac{1}{2d-1}. \quad (14)$$

The n th derivative of $f(x)$ at point x_0 is

$$f^{(n)}(x_0) = -\frac{d(2d-1) \cdots (2d-n+1)}{\sigma^2} x_0^{2d-n}. \quad (15)$$

Then a Taylor series for the function $f(x)$ at point x_0 can be written as

$$f(x) = f(x_0) - \frac{(\sigma^2 p)^{2d\alpha}}{\sigma^2} g\left(\frac{x-x_0}{x_0}\right), \quad (16)$$

where

$$g\left(\frac{x-x_0}{x_0}\right) = \sum_{n=2}^{\infty} \frac{d^{-\alpha}}{n!} (2d-1) \cdots (2d-n+1) \left(\frac{x-x_0}{x_0}\right)^n. \quad (17)$$

The moments can now be estimated as

$$\langle M^p \rangle \sim e^{ap+f(x_0)} \int_{-\infty}^{\infty} \exp\{-hg[(x-x_0)/x_0]\} dx, \quad (18)$$

where

$$h = \frac{1}{\sigma^2} (\sigma^2 p)^{2d\alpha}. \quad (19)$$

Let us introduce the variable

$$y = \frac{x-x_0}{x_0}. \quad (20)$$

Then we can rewrite the representation (18) as

$$\langle M^p \rangle \sim x_0 e^{ap+f(x_0)} \int_{-\infty}^{\infty} \exp[-hg(y)] dy. \quad (21)$$

Now the function

$$g(y) = \sum_{n=2}^{\infty} \frac{d^{-\alpha}}{n!} (2d-1) \cdots (2d-n+1) y^n \quad (22)$$

is independent of σ and p , i.e., this function is independent of the parameter h (for a fixed value of the branching dimension d). For large h , i.e., for

$$h \gg 1, \quad (23)$$

the integral in the right-hand side of Eq. (21) is dominated by $\min_y\{g(y)\}$, i.e.,

$$\langle M^p \rangle \sim x_0 e^{ap+f(x_0)} e^{-h \min_y\{g(y)\}}. \quad (24)$$

Since for $2d-1 > 0$ the real function $f(x)$ has generally one maximum at the point x_0 only, this is the absolute maximum of this function, and, therefore, $g(y) \geq 0$. Hence, $\min_y\{g(y)\} = 0$ and we obtain from Eq. (24)

$$\langle M^p \rangle \sim x_0 e^{ap+f(x_0)}. \quad (25)$$

It is easy to show using Eqs. (19) and (23) that for

$$\sigma^2 > \left(\frac{2d}{(2d-1)^2 e}\right)^{2d} \quad (26)$$

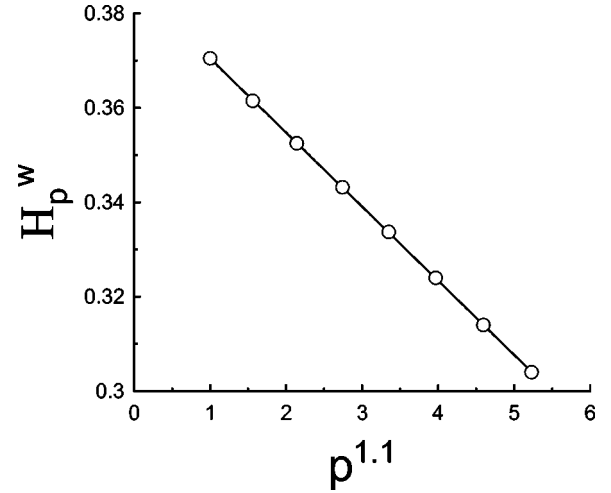


FIG. 2. H_p^w versus $p^{1.1}$ for $E_d = 1$ eV. The straight line (best fit) indicates agreement between the data and Eq. (30) with $\alpha = 1.1$ (which corresponds to the analytic branching cascade with branching dimension $d \approx 0.95$).

we can neglect the multiplier x_0 in comparison with the exponent in the right-hand side of representation (25), and we obtain from (25)

$$\langle M^p \rangle \sim \exp[ap + p(1-1/2d)(\sigma^2 p/d)^\alpha]. \quad (27)$$

Using Eq. (27) we then obtain a generalized scaling relationship based on the stretched log-normal distribution,

$$\frac{\langle M^q \rangle}{\langle M^z \rangle^{q/z}} \sim \left(\frac{\langle M^p \rangle}{\langle M^z \rangle^{p/z}} \right)^{q(\alpha-z^\alpha)/p(p^\alpha-z^\alpha)}. \quad (28)$$

Substituting Eqs. (4) and (5) into Eq. (28) we obtain the relationship

$$\frac{r^q H_q^w}{r^q H_z^w} \sim \frac{r^q H_p^{w(q^\alpha-z^\alpha)/(p^\alpha-z^\alpha)}}{r^q H_z^{w(q^\alpha-z^\alpha)/(p^\alpha-z^\alpha)}}$$

and then the functional equation for H_p^w

$$\frac{H_q^w - H_z^w}{H_p^w - H_z^w} = \frac{q^\alpha - z^\alpha}{p^\alpha - z^\alpha}. \quad (29)$$

The general solution of this equation is

$$H_p^w = a + bp^\alpha, \quad (30)$$

where a and b are some constants.

Figures 2 and 3 show the wavelet Hurst exponents H_p^w calculated using the data obtained in Ref. [5] for two values of $E_d = 1$ eV and ∞ eV, respectively (the value $E_d = \infty$ eV corresponds to the case when desorption is forbidden). In these figures the horizontal axes are chosen to provide comparison with the representation (30). The straight lines (best fit) are drawn to indicate consistency of the data with the stretched log-normal distribution. For $E_d = \infty$ the parameter $\alpha \approx 1.3$ and, consequently, the branching dimension d

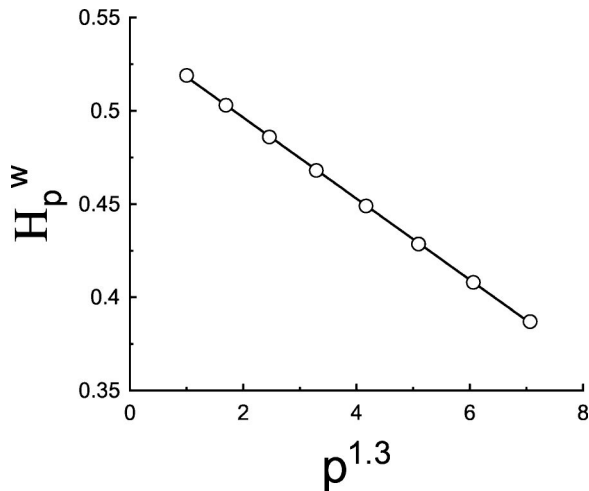


FIG. 3. H_p^w versus $p^{1.3}$ for $E_d = \infty$. The straight line (best fit) indicates agreement between the data and Eq. (30) with $\alpha = 1.3$ (which corresponds to the analytic branching cascade with branching dimension $d \approx 0.88$).

≈ 0.88 , while for $E_d = 1$ eV the parameter $\alpha \approx 1.1$ and the branching dimension $d \approx 0.95$.

Finally, it should be noted that different probability distributions can lead to the same relationships between moments. In particular, the stable Levy laws lead formally to the same relation (30) as the stretched log-normal distribution. However, for the stable Levy laws a strong restriction on the parameter α , $\alpha \leq 1$, appears as a necessary condition (see, for instance, [12]). Since, in the case considered above, we ob-

tained $\alpha > 1$ one can conclude that for kinetic surface roughening we are dealing with the stretched log-normal distribution for which (in contrast with the stable Levy laws) the parameter α can take values larger than 1.

IV. DISCUSSION

Since for $E_d = 1$ eV the value of the exponent $\alpha \approx 1.1$ is not far from its log-normal value $\alpha = 1$, the difference between these values of α should be compared with the accuracy of the calculations of τ_p in Ref. [5]. At the value of $E_d = 1$ eV the maximum error of the calculations of τ_p in Ref. [5] is about 1%. This accuracy allows us to be confident that even for $E_d = 1$ eV the simple log-normal state is still not reached. It is an interesting problem for future simulations to check whether for $E_d < 1$ eV we can reach the log-normal state.

In Ref. [5], τ_p was calculated for both positive and negative p . However, we can use only the data for positive values of p because the calculations performed in Sec. III allow us to operate with negative values of p for integer branching dimensions only (which is not the case here). Expansion of the method suggested in Sec. III to negative values of p also seems to be an interesting problem for future investigations.

ACKNOWLEDGMENTS

The author is grateful to M. Ahr for providing his data (with M. Biehl), to T. Nakano for discussions, and to the Machanaim Center (Jerusalem) and the Graduate School of Science and Engineering of the Chuo University (Tokyo) for support.

-
- [1] A.-L. Barabási and H. E. Stanley, *Fractal Concepts in Surface Growth* (Cambridge University Press, Cambridge, 1995).
 [2] A. Kundagrami, C. Dasgupta, P. Punyindu, and S. Das Sarma, *Phys. Rev. E* **57**, R3703 (1998).
 [3] J. Krug, *Phys. Rev. Lett.* **72**, 2907 (1994); *Adv. Phys.* **46**, 139 (1997).
 [4] N. Decoster, S. G. Roux, and A. Arnéodo, *Eur. Phys. J. B* **15**, 739 (2000).
 [5] M. Ahr and M. Biehl, *Phys. Rev. E* **62**, 1773 (2000).
 [6] A. Bershadskii, T. Nakano, D. Fukayama, and T. Gotoh, *Eur.*

- Phys. J. B* **18**, 95 (2000).
 [7] A. C. Monin and A. M. Yaglom, *Statistical Fluid Mechanics 2* (MIT Press, Cambridge, MA, 1975).
 [8] K. R. Sreenivasan, *Annu. Rev. Fluid Mech.* **23**, 539 (1991).
 [9] E. Bacry, J. M. Muzy, and A. Arnéodo, *J. Stat. Phys.* **70**, 635 (1992).
 [10] S. Das Sarma, C. J. Lanczycki, R. Kotlyar, and S. V. Ghaisas, *Phys. Rev. E* **53**, 359 (1996).
 [11] A. Bershadskii, *Europhys. Lett.* **39**, 587 (1997).
 [12] D. Schertzer and S. Lovejoy, *Physica A* **185**, 187 (1992).